CORTEX 97 (2017) 32–48

Available online at www.sciencedirect.com

ScienceDirect

Journal homepage: www.elsevier.com/locate/cortex

Research report

Strategic adaptation to non-reward prediction error qualities and irreducible uncertainty in fMRI☆

Daniel S. Kluger [a,b,*] *and Ricarda I. Schubotz* [a,b,c]

[a] *Department of Psychology, University of Muenster, Muenster, Germany*
[b] *Otto-Creutzfeldt-Center for Cognitive and Behavioral Neuroscience, University of Muenster, Muenster, Germany*
[c] *Department of Neurology, University Hospital Cologne, Cologne, Germany*

ARTICLE INFO

Article history:
Received 15 February 2017
Reviewed 22 May 2017
Revised 19 July 2017
Accepted 11 September 2017
Action editor Pia Rotshtein
Published online 3 October 2017

Keywords:
fMRI
Expectation
Prediction error
Sequence learning
Top-down control

ABSTRACT

Prediction errors are deemed necessary for the updating of internal models of the environment, prompting us to stop or assert current action plans and helping us to adapt to environmental features. The aim of the present study was twofold: First, we sought to determine the neural underpinnings of qualitatively different abstract prediction errors in a serial pattern detection task. Distinct frontoparietal components were found for sequential terminations (inferior frontal gyrus – IFG) and extensions (superior frontal sulcus, posterior cingulate cortex, and angular gyrus), respectively. These findings provide a novel approach of distinguishing non-reward prediction error signals with regard to behavioural consequences they entail.

Second, we investigated predictive processing as a function of statistical context (*irreducible uncertainty*). We hypothesised that the prospective scope of model-based expectancies is adapted to the stability of respective contexts in that unstable environments call for more frequent comparisons of expectancies with sensory input, resulting in stepwise predictions. Changes in environmental stability were reflected in activation of the angular gyrus and IFG for the highly uncertain context at potential points of prediction violation (*checkpoints*). Notably, this effect was not due to local fluctuations in stimulus improbability (*surprise*). Although further behavioural support is needed, data point towards a context-dependent adaptation of predictive strategies. Conceivably, enhanced neural responses at sequential checkpoints could reflect stepwise rather than full-length prediction. This strategic adjustment presumably relies on the iterant evaluation of model information retrieved from working memory, as suggested by strengthened functional connectivity of the parahippocampal area during epochs of high uncertainty.

☆ The reported work was performed at Department of Psychology, University of Muenster, Fliednerstr. 21, D-48149 Muenster, Germany.

* *Corresponding author*. Department of Psychology, University of Muenster, Fliednerstr. 21, D-48149 Muenster, Germany.
E-mail address: daniel.kluger@uni-muenster.de (D.S. Kluger).

https://doi.org/10.1016/j.cortex.2017.09.017
0010-9452/

1. Introduction

In attempting to make sense of incoming sensory event information in everyday life, we are constantly faced with discrepancies between our internal model of the world and the information we actually obtain (Rao & Ballard, 1999). In predicting future events, the brain efficiently processes predictable portions in perceptual information: only if incoming sensory signals differ from higher-level predictions is the corresponding error signal propagated "upward" to the next highest stage of the processing hierarchy (Friston, 2005; Mumford, 1992). Such prediction errors inarguably differ with regard to their quality and the behavioural consequences they entail: when walking down a familiar flight of stairs, one might occasionally over- or underestimate the remaining number of stairs on the bottom landing, evoking qualitatively different moments of surprise. Furthermore, context will likely influence the way in which we make assumptions about upcoming events: we will compare our expectations with reality more frequently in noisy or unfamiliar contexts, for instance when carrying a fridge through the same staircase in dim lighting.

Research on definitive features of these prediction errors has predominantly been directed towards quantitative rather than qualitative differences between neural error signals. For instance, the concept of *surprise* (Jones, 1979), cast to reflect the improbability of a particular event, has been demonstrated to modulate prediction errors in that more surprising expectancy violations elicit stronger error signals (Egner, Monti, & Summerfield, 2010; Strange, Duggins, Penny, Dolan, & Friston, 2005). However, aside from a few studies in the cognitive (e.g., Den Ouden, Daunizeau, Roiser, Friston, & Stephan, 2010; Schiffer, Ahlheim, Wurm, & Schubotz, 2012) and the perceptual domain (O'Reilly et al., 2013), imaging efforts to classify *qualitatively* different types of such prediction errors have so far been restricted to contexts involving a reward component. Here, findings from animal studies (Bayer & Glimcher, 2005) and gambling tasks in humans (Delgado, Locke, Stenger, & Fiez, 2003) have demonstrated a functional distinction of *positive* and *negative* reward prediction errors based on whether an obtained reward value was higher or lower than expected, respectively (Schultz et al., 1998).

In contrast, such distinctive characteristics of prediction errors are considerably less well understood in absence of external reward (note that predicting or responding correctly may be rewarding in its own right (Holroyd & Coles, 2002), which is not the objective of the present study). In light of the immediate importance of error signals for internal model updating (e.g., Bastos et al., 2012) and adequate action selection, however, the need to understand the qualities of more abstract prediction errors becomes evident: as prediction errors are thought to be the foundation of learning mechanisms (Den Ouden, Friston, Daw, McIntosh, & Stephan, 2009), different types of expectancy violations might result in qualitatively distinguishable prediction error signals and – consequently – in distinct modifications of upcoming expectancies and behaviour. Recall that short term predictions are used to facilitate perception when we observe structured regularities such as sequential events. When these regularities end earlier than expected, the appropriate adaptation would be to reject the now invalid predictive model in favour of a more *externally* driven mode of tracking incoming information. In contrast, any regularity we perceive may as well persist longer than expected. Accordingly, such an unexpected extension would then call for a resumption of the *internally* driven mode of model-based prediction.

As much as this reactive, local adaptation of stimulus processing and behaviour should reflect different types of prediction errors, it should likewise depend on global, higher order characteristics of the environment. Exploring the nature of error signals and their effects on model adaptation therefore raises the question of whether predictive strategies remain constant across contexts. Different measures of uncertainty have been discussed to refer to the variability of informational value over time, thus reflecting higher-order statistical features of the environment (Bland & Schaefer, 2012; Yu & Dayan, 2005). While sensitivity to context uncertainty has been linked to activity in the anterior cingulate cortex (ACC) as a function of reward prediction error computation (Behrens, Woolrich, Walton, & Rushworth, 2007; Scholl et al., 2017; Silvetti, Seurinck, & Verguts, 2013), implications of context (in)stability on abstract prediction still remain unclear. Therefore, we manipulated the composition of experimental blocks to vary the amount of *irreducible uncertainty* (Payzan-LeNestour & Bossaerts, 2011; De Berker et al., 2016) that would remain after successful learning. Conceivably, memory-driven internal models of future sensory information might be adapted to the uncertainty of respective contexts: in stable contexts of low uncertainty, prediction errors can be conceived of as more meaningful in that they are highly informative with regard to potential benefits of model adaptation (i.e., learning). In contrast, prediction errors in statistically unstable (i.e., highly uncertain) contexts carry less information contributing to learning-related gains. Predicting upcoming events can be considered an investment in the sense that false predictions inevitably lead to costly adjustments of forward models (Clark, 2013). Therefore, depending on how reliably forward models can be used to predict future events (as conveyed through statistical learning of environment regularities), it may be more efficient to employ a strategy of partial or stepwise short-term predictions rather than predicting consecutive events at full length. For example, as opposed to preparing a complete model of an expected sequence of events, a stepwise prediction might imply an iterative monitoring of sequence continuation at particular sequential positions. Research on sequential actions has suggested *decision points* (Norman, 1981; Reason, 1992) as points in time where the selection of appropriate actions requires accessing information about the broader task context. Translated into the perceptual primacy of our experimental paradigm, we propose *checkpoints* as equally informative sequential positions at which broader, uncertainty-dependent contextual information is exploited to prompt strategic adjustments. Most likely to serve as such checkpoints would be those points in time where the occurrence of stimuli was probabilistically modulated by blockwise manipulation of irreducible uncertainty. This way, statistical learning might be employed to adapt predictive strategies to particular

informational structures in the environment. Support for this hypothesis comes from studies linking the working memory network (most prominently hippocampus and adjacent areas) to both the predictive processing of sequential patterns (Fortin, Agster, & Eichenbaum, 2002; Lisman, 2009; Rolls, 2013) as well as the decoding of contextual information (Allen, Salz, McKenzie, & Fortin, 2014; Davachi & DuBrow, 2015).

We conducted the present functional magnetic resonance imaging (fMRI) study to assess qualitative differences between prediction error signals and the influence of uncertainty on predictive strategies using an implicit cueing paradigm. Participants were asked to detect short or long ordered digit sequences (5 and 7 items, respectively) within an otherwise pseudorandom stream of single digits. They indicated the onset of a detected sequence by an immediate button press and the sequence ending by button release. The expected sequence length, as implicitly cued by digit colour (see Material and methods), was occasionally violated by terminations and extensions. Thus, whereas the task was overtly concerned with sequence detection, our analysis was focussed on specific events during or at the end of sequences.

As to our first hypothesis, we expected distinguishable neural correlates to reflect the respective reorientation towards external stimuli (sequential terminations) or towards the internal model derived from working memory (sequential extensions). Particularly, the unexpected need to disregard the currently employed internal model as induced by sequential terminations was hypothesised to engage the inferior frontal gyrus (IFG), an area that has been reported for violations of ordered pattern expectancy across domains (Fiebach & Schubotz, 2006).

Second, we assessed the effects of context uncertainty on predictive strategies by manipulating the proportion of violated sequences over time. Neural activity at checkpoint positions was expected to be elevated in highly uncertain contexts, thus indicating a stepwise prediction mode. Due to its established role in reward-related uncertainty monitoring (specifically *volatility*, Behrens et al., 2007), we assumed ACC to represent higher-level context information necessary to initiate stepwise predictions in highly uncertain environments. Crucially, these global fMRI effects were controlled for potential confounds by varying levels of stimulus-bound surprise (i.e., the extent to which individual stimuli were locally unexpected). To this end, we employed a parametric regressor of nuisance reflecting a stimulus' respective surprise value, thus allowing us to disentangle higher level context effects from mere differences in improbability.

2. Material and methods

2.1. Participants

A total of 22 neurologically healthy, right-handed volunteers (13 female, mean age: 24.3 (20–30) years) participated in the study. Participants were recruited from the university's volunteer database and had normal or corrected-to-normal vision. Colour blindness was ruled out using Ishihara colour test plates (Ishihara, 1917). Written informed consent was obtained from each participant prior to the start of experimental procedures. Experimental standards complied with the local Ethics Committee of the University of Münster. Participants selectively received payment or course credit as compensation for their participation in the study. Two participants were excluded from further data analysis due to poor behavioural performance and self-reported tiredness during the experiment (see below). Therefore, all reported analyses of functional data are based on a sample of 20 participants (12 female, mean age 24.8 (21–30) years).

2.2. Stimulus material

The stimuli consisted of pseudorandomly coloured single digits (0–9, size 1.5° of visual angle) presented individually for 500 ms in the centre of a light grey computer screen (see Fig. 1A). Digits were presented in blocks with a length of approximately 6 min. Numbers of presentations for all colours and digits were equally distributed both within and across blocks. Each block contained *sequential trials* (i.e., digits with a recognisable relation to the preceding one) as well as *random trials* (i.e., digits that were not discernibly related to either the preceding or the following digit). Sequential trials in turn belonged to one of two types of sequences: *ordered sequences* constantly increased the preceding figure by one (e.g., 5–6 – 7–8 – 9; Fig. 1A, left). In order to allow for ordered sequences to start on any figure, the ascending regularity necessarily included the 0 character and was thus continued in a circular fashion after the figure 9 (e.g., 8–9 – 0–1 – 2). *Colour sequences* were defined as consecutive trials all presented in the same colour (dark red). Importantly, the numerical values during colour sequences were pseudorandom (Fig. 1A, right). Therefore, at no point was there a succession of continuously ascending figures presented in the same colour, but only one sequential condition at a time (i.e., ordered or colour). Colour sequences were employed to ensure a high level of attentiveness and were not a pivotal subject to our analyses. Random trials included neither self-repetitions nor immediately adjacent figures and therefore could not be mistaken for ordered sequences.

Undisclosed to the participants, two colours were used as cues to indicate the onset of ordered sequences: one colour marked the first digit of a *short* ordered sequence (regular length of five digits), a second colour marked the first digit of a *long* ordered sequence (regular length of seven digits). Each participant was assigned two individual cue colours which did not belong to the same hue. Cue validity was fixed at $p = .80$ throughout the experiment with invalid cues being followed by a random figure instead of the next higher one (as would have been suggested by the cue). Neither one of the cue colours nor the red hue used for the colour sequences appeared during random trials. Importantly, the colour cues were employed to trigger predictions with regard to the length of the to-be-observed sequence and were not analysed as events of interest themselves. Implicit cues were used to control for mere attentional effects and to keep participants focussed on the numeric information (instead of the colour information) while tracking the digits for regularities.

In order to induce prediction errors based on the implicit information conveyed by the colour cues, ordered sequences were manipulated in terms of their *expectation compliance*. This

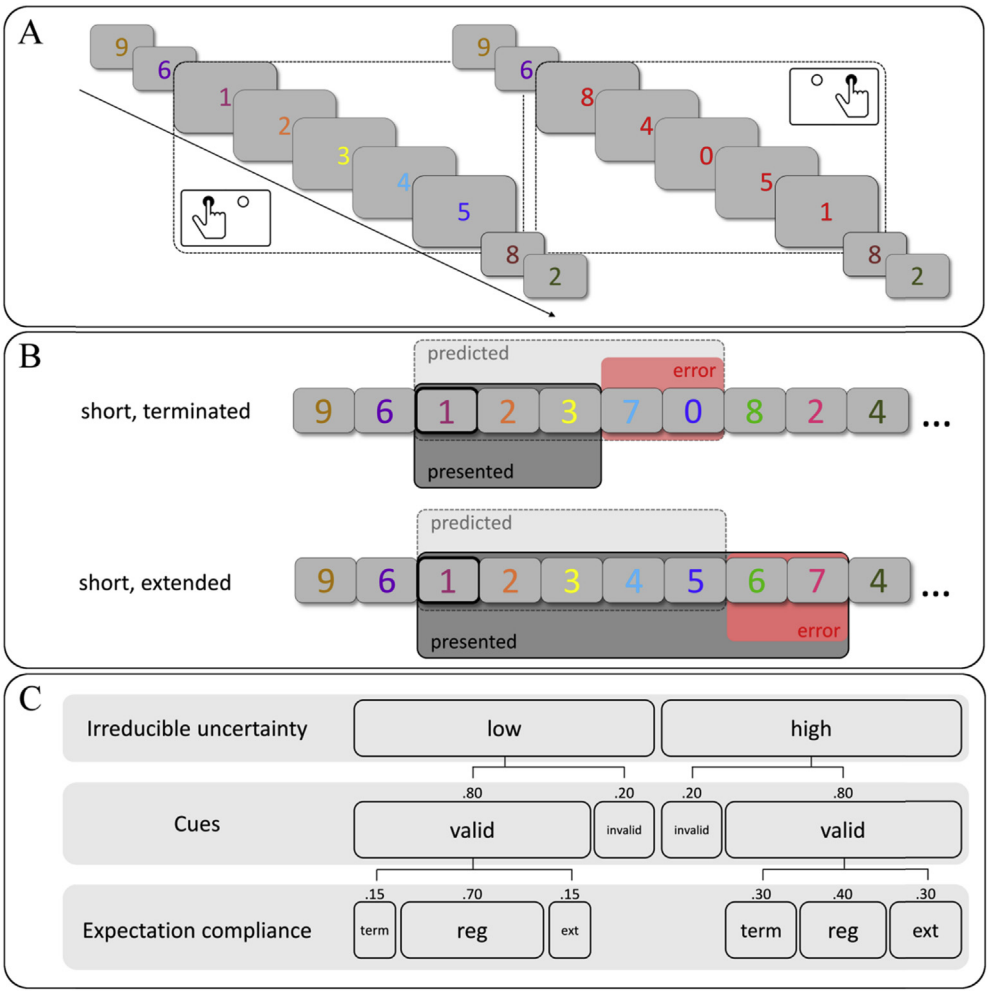

Fig. 1 – (A) Exemplary trial successions and time windows of respective corresponding responses for ordered (left) and colour sequences (right). Sequential trials have been highlighted for illustrative purposes. (B) Cue-based expected sequence length and resulting prediction errors for terminated, and extended short ordered sequences (*expectation compliance*). Based on the cue (in this case, a magenta figure), five regularly ascending figures are expected. Cue trial has been highlighted for illustrative purposes. Top: terminated sequences are shortened by two trials and therefore induce a prediction error (predicted sequence > presented sequence). Bottom: extended sequences are prolonged by two trials and therefore induce a prediction error (predicted sequence < presented sequence). (C) Local transition probabilities for terminated, regular, and extended sequences depending on respective block uncertainty. Note that only the composition of expectation compliance levels varied with uncertainty while cue validity itself remained fixed across blocks.

factor was introduced to distinguish between *regular*, *terminated*, and *extended* ordered sequences. Given the regular length of five and seven figures, respectively, terminated sequences were shortened by two items (e.g., three instead of five figures for short ordered sequences) while extended sequences were equally prolonged by two items (e.g., seven instead of five figures for short ordered sequences). A graphic display of expected sequence length and expectation compliance is shown in Fig. 1B.

Finally, the composition of regular, terminated, and extended sequences within a particular block was varied across blocks. This way, the *irreducible uncertainty* of the blocks (i.e., the frequency of change with regard to cue-based expectations) was set to be either *high* or *low*. Blocks of low uncertainty featured local probabilities of $p_{reg} = .70$ for the regular configuration and $p_{term/ext} = .15$ for both terminated and extended sequences. These blocks could therefore be seen as statistically stable regarding cue-based expectations. Local probabilities for terminated and extended sequences were always identical for both sequence lengths. Highly uncertain blocks, in contrast, corresponded to a more unstable statistical structure regarding the expectation based on the cue. Local probabilities after the cue during highly uncertain blocks were $p_{reg} = .40$ and $p_{term/ext} = .30$. It is important to note that at any point during the experiment the regular configuration was the statistically most likely continuation of the sequence. An overview of the statistical structure following the uncertainty factor is provided in Fig. 1C, please see the

Supplementary material for details on the composition of experimental blocks.

Starting points of all sequences were balanced across digits. Successions of random trials were equally distributed within a range of 5–9 digits ($M = 7.19$ digits) both within and across blocks. To ensure an even distribution of colour presentations, a total of 29 different colours were used. The colours employed in the present study had been validated in a behavioural pilot study ($n = 18$) to ensure equal visibility of all colours.

2.3. Tasks

Participants were asked to indicate detection of ordered sequences as well as colour sequences by corresponding button presses. Therefore, they were instructed to press the left button with their right index finger as soon as they noticed an ordered sequence and to hold the button for the duration of the sequence. Accordingly, release of the left mouse button was to indicate the end of the ordered sequence (i.e., the onset of subsequent random trials). Equivalently, participants were instructed to press and hold the right mouse button with their right middle finger to indicate detection of a colour sequence. Once again, release of the right mouse button marked the end of a colour sequence. A mouse was used in the behavioural sections (i.e., introductory trials, training, and post-measurement) to closely match responses with the two-button response box used during the fMRI session (see below).

2.4. Experimental procedures

The study was conducted on two consecutive days. The first day appointment was laid out as a training session in order to allow participants to familiarise themselves with the task and to provide them with implicit knowledge concerning the cues and the underlying statistical structure of the experiment. Importantly, at no point during the training or the fMRI session was it revealed that there was informational content in some of the colours (i.e., the cues) or that the blocks varied in their respective statistical structure (i.e., their level of uncertainty). The second day included the fMRI session as well as a subsequent post-measurement. The experiment was programmed and run using the Presentation 14.9 software (Neurobehavioral Systems, San Francisco, CA, USA).

2.5. Day 1 (training session)

After having been informed about the very general scope of the study ("digit processing", supposedly), participants completed a first introduction to the task. Participants were shown a 1 min stream of digits including exactly one presentation of each ordered sequence configuration (i.e., terminated, regular, and extended sequences of both lengths), one invalid cue of each sequence length as well as one colour sequence. Length range and proportion of random trials were matched with the behavioural and the fMRI experiment. Responses were not recorded during the introductory trials and participants were allowed to repeat the introduction until they felt comfortable with the task.

The training consisted of two blocks (one block of high and low uncertainty, respectively) with a total duration of approx. 12 min – (for more details, see section "Stimulus material"). Block order was balanced across participants. Length range and proportion of random trials were matched with the fMRI experiment. After the completion of a block, participants were encouraged to take some time and grant themselves a short break before continuing with the next block.

2.6. Day 2 (fMRI session and post-measurement)

Participants once again completed the introductory phase from the previous day in a quiet working environment immediately before entering the scanner. The following fMRI session consisted of four blocks (two blocks of both high and low uncertainty, respectively) with a total duration of approx. 24 min. Contrary to the training, participants were presented with a screen notifying them of a short break for ten seconds after completion of a block. Experimental procedure and task during the fMRI session were otherwise identical to the training session.

Following the functional scanning, participants completed a behavioural post-measurement in order to assess their implicit knowledge of the cue information. To this end, they were presented with one experimental block (duration approx. 5 min) shown on a computer. Length range and proportion of random trials were matched with the training session and the fMRI experiment. Participants were asked to perform the identical task as before (i.e., to indicate sequence detection by button press). Crucially, only half of the ordered sequences were cued by the same colours as during the training and the fMRI session. The other half began with fixed but different colours that had indeed been presented during training and fMRI, but not as cues for the respective participant. Therefore, they contained no implicitly learned information concerning upcoming trials. As with the established cue colours, two previously non-informative colours were assigned to mark the beginning of short and long ordered sequences, respectively.

Finally, participants were interviewed verbally to assess whether they were aware of any regularity at all with regard to the digits' colours. All participants denied having noticed any colour-related regularity.

2.7. Behavioural data analysis

Statistical analyses of behavioural responses were performed using R statistical software (R Foundation for Statistical Computing, Vienna, Austria). If not stated otherwise, an α-level of .05 was defined as a statistical threshold.

First, correct and incorrect responses were aggregated separately for training, fMRI session, and post-measurement for each participant. Incorrect responses were further divided into misses (no response over the course of a sequence) and false alarms (response occurring without presentation of sequential trials). Participants' overall performances were assessed via the discrimination index (PR; Snodgrass & Corwin, 1988), defined as the difference between hit rate and false alarm rate: correctly reported sequences (i.e., ordered or colour sequences) relative to all

sequences was defined as the hit rate. The false alarm rate was defined as falsely reported sequences (again, ordered or colour sequences) relative to all sequences. No specific time-out criterion was defined for the onset of button presses, i.e., responses were registered throughout the whole length of the respective sequence.

Reaction times for button presses (onset latency) and releases (offset latency) were assessed for fMRI session and post-measurement. Latencies were aggregated separately for the levels of *expectation compliance* (terminated, regular, extended) and *uncertainty* (high, low) as well as for established versus new cue colours, respectively. Onset latency was calculated as reaction time relative to the onset of the second trial of any particular ordered sequence: the second trial of the sequence was the earliest possible point to detect a sequential pattern, since the current trial always had to be compared to the preceding one (i.e., to check whether the figure had risen by 1). Offset latency was calculated as reaction time relative to the onset of the first random trial after any particular sequence. Repeated-measures analyses of variance (ANOVA) and paired *t*-tests were used to assess possible differences in offset (depending on expectation compliance and uncertainty) and onset latency (learned *vs* new cue colours during post-measurement), respectively. Where appropriate, results of the paired *t*-tests were corrected for multiple comparisons at $p = .05$ using the false discovery rate (fdr) correction by Benjamini and Hochberg (1995).

2.8. Functional data analysis

2.8.1. fMRI data acquisition and data preprocessing

Functional and structural imaging data were collected using a 3T Siemens Magnetom Prisma scanner (Siemens, Erlangen, Germany) equipped with a 20-channel head coil. Participants lay supine with their right hand placed on a two-button response box. Index and middle finger were placed on the two response buttons, matching the response contingencies from the training session. Participants' arms were stabilised on form-fitting cushions and foam padding around the head was applied to prevent motion artefacts. Earplugs and noise-cancelling headphones were provided to reduce scanner noise.

During functional imaging, 30×4 mm axial slices (1 mm spacing, 64×64 voxel matrix, 192×192 mm field of view, resulting voxel size $3 \times 3 \times 5$ mm) were acquired parallel to the bi-commissural line (AC-PC) using a single-shot gradient echo-planar imaging (EPI) sequence sensitive to blood oxygenation level dependent contrast (BOLD, TR = 2000 ms, TE = 30 ms, 90° flip angle, ascending recording, 800 repetitions). Prior to the functional session, a high-resolution structural scan was recorded for each participant using a standard Siemens 3D T1-weighted whole brain MPRAGE imaging sequence ($1 \times 1 \times 1$ mm voxel size, TR = 2130 ms, TE = 2.28 ms, 256×256 mm field of view, 192 sagittal slices).

Data processing was done with the Lipsia software package (Lohmann et al., 2001). Functional data were spike-corrected (using interpolation with adjacent time points) to reduce artefacts within time series. Correction for slice acquisition time (using cubic spline interpolation) and head motion (3 translation, 3 rotational parameters) was applied and functional data were co-registered with the structural scan (using rigid transformation). Individual structural scans were normalised to the MNI template via general affine transformation and resulting parameters were applied to the functional scans. The resulting normalised functional images were resampled to 3 mm isotropic voxels, high-pass filtered with a 100 sec period cutoff and spatially smoothed with an 8 mm full-width half-maximum (FWHM) Gaussian kernel.

2.8.2. fMRI analysis

Event-related BOLD responses were estimated in a general linear model (GLM) approach. The GLM was constructed to test for distinct neural correlates of the different error types as well as for effects of statistical block structure on neural processing at different time points during ordered sequences. Additionally, the parametric effect of surprise was modelled to control for trial-by-trial variation in stimulus improbability. Therefore, the model comprised a total of seven regressors of interest reflecting the 3×2 combination of the factors *expectation compliance* (terminated, regular, extended) and *uncertainty* (low, high) plus the surprise parameter. Regressors of nuisance included experimental breaks, colour sequences, and motor responses (button presses and releases) in order to account for variance unrelated to the events of interest.

For terminations, the event onset was time-locked to the first unexpected *random* digit (i.e., the fourth [short sequences] or sixth [long sequences] sequential position, respectively; see Fig. 1B). Equivalently, extensions were modelled with the onset time-locked to the first unexpected *sequential* digit (i.e., the sixth [short] or eighth [long] sequential position, respectively). Regular events (termed *checkpoints*) were defined as points in time at which we hypothesised the incoming stimulus to be checked for either a termination (i.e., a check occurring during the ongoing sequence) or an extension (i.e., a check at the regular end) of the ordered sequence. Importantly, checkpoints were only classified as such when the ordered sequence was in fact continued as indicated by the cue, that is, in the regular configuration (see Fig. 2 for an example and Supplementary Fig. S1 for details on event specification). In case the current stimulus did not match the prediction, the event was classified as a prediction error instead of a checkpoint.

With respect to difference characteristics, one could justifiably argue that the difference between checkpoints and prediction errors may not at all be qualitative, but rather a quantitative excess of prediction errors with regard to their respective improbabilities. From this point of view, checkpoints could be construed as muted prediction error signals with a lesser degree of surprise. While surprise inarguably modulated cognitive processing in the present task, our key point of suggesting a functional role for checkpoints was to gain insight into qualitatively different processing of regular events depending on the particular context. By including a parametric surprise regressor, we attempted to discriminate between these qualitative effects and quantitative distinctions that can be ascribed to mere differences in improbability.

The parametric effect of surprise was estimated following the notion of an ideal Bayesian observer (see Harrison,

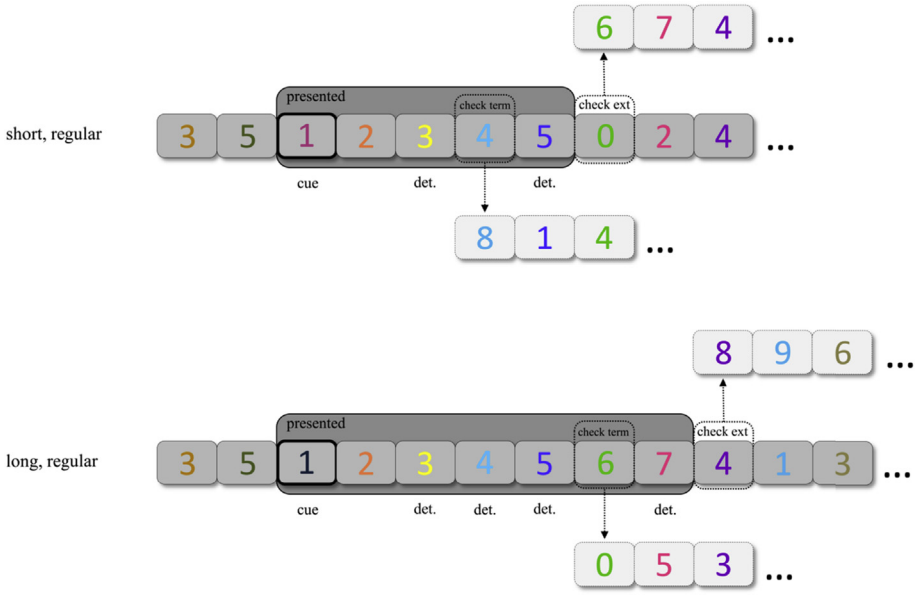

Fig. 2 – Illustration of checkpoints during a regular short and long ordered sequence, respectively. As indicated by the cue (highlighted for the purpose of this graphic), five or seven consecutive digits following the +1 rule are presented. Two checkpoints are hypothesised over the course of each sequence: For instance, during short ordered sequences (top), the fourth item can be used to check whether the sequence is terminated (check term) or not. A hypothetical course of a terminated sequence is outlined (lower trial succession, dashed framing). The sixth item (i.e., the first random figure after the regular short ordered sequence) can be used to check for an extension of the sequence (check ext). A hypothetical course of an extended sequence is outlined (upper trial succession, dashed framing). Within a particular ordered sequence, checkpoints are always preceded by deterministic items (det.).

Duggins, & Friston, 2006). Event-specific surprise $I(x_i)$ was defined as the improbability of event x_i, i.e.,

$$I(x_i) = -\ln p(x_i)$$

with

$$p(x_i) = \frac{n_j^i + 1}{\sum_k n_k^i + 1}$$

where n_j^i denotes the total number of occurrences of outcome j (*terminated, regular, extended*) up to the current observation i relative to the sum of all past observations (with k for all possible outcomes).

2.9. Contrast specification

The main effect of *expectation compliance* was assessed by the second-level contrast of terminated and extended sequences (TERM > EXT). Common activations of both prediction error types were assessed by the conjunction of the two single contrasts versus checkpoints, respectively (i.e., TERM > CHECK ∩ EXT > CHECK). Note that due to the probabilistic structure of the task, there were considerably more checkpoints than prediction errors contributing to the respective regressors (ratio ~ 2:1). Therefore, for the conjunction of TERM > CHECK and EXT > CHECK, we constructed a parallel GLM identical to the one described above, with the one exception that only half of the checkpoint events were included in the respective regressors of the second model. While this approach resulted in reduced power of the respective contrasts and their conjunction, its merit lies in a markedly well-balanced, less biased contrast of conditions.

The effects of *uncertainty* on checkpoint and prediction error processing were assessed by the contrasts of high versus low uncertainty checkpoints (CHECK_HIGH > CHECK_LOW) and prediction errors (PE_HIGH > PE_LOW, data not shown), respectively.

For group level analyses, one sample *t*-tests were calculated using first-level contrast images of all participants. Resulting t-values were converted to z-scores and thresholded at voxel-wise $p < .001$. In a second step, this initial thresholding was combined with a cluster-extent based threshold derived from Monte Carlo Simulation (see Forman et al., 1995). We ran 5000 iterations using the fMRIMonteCluster tool (available at github.com/mbrown/fmrimontecluster), yielding a cluster-extent based threshold of $k > 783$ mm^3 (29 contingent voxels, cluster-level $p < .05$).

2.10. Exploratory functional connectivity analyses

2.10.1. Eigenvector centrality mapping

When investigating the interplay of brain regions in forming coactivation networks, functional connectivity measures have become increasingly popular to complement BOLD amplitude effects of participating brain regions. Eigenvector

centrality mapping (ECM) has been proposed by Lohmann et al. (2010) as a graph-based means to determine the centrality of neural structures within their respective networks. Particularly, eigenvector centrality (Bonacich, 2007) refers to how strongly a certain structure (a *node*, in terms of graph theory) is functionally connected to other highly interconnected nodes. Therefore, both number and quality of connections are factored into the centrality value assigned to a particular voxel. Since the interesting aspect here was precisely to evaluate the influence of irreducible uncertainty on the neural processing within task-related networks (whose components are themselves highly interconnected), ECM was explicitly well suited for the functional connectivity analysis at hand. Importantly, ECM does not depend on a priori assumptions and, due to computational efficiency, allows for functional connectivity analyses of the entire brain. Finally, ECM does not require parameter adjustments other than the definition of the voxel space and the time period of interest.

In order to assess potential effects of uncertainty on functional connectivity, eigenvector centrality was analysed post-hoc within a whole-brain mask (≈60 000 voxels). To avoid connectivity changes caused by the mere duration of scanner time (see Lohmann et al., 2010), ECM analysis was restricted to the first half of the experiment (i.e., one block of each uncertainty level in counterbalanced order) for each participant. Pairwise similarity matrices for time series of any two voxels were computed and subsequently analysed by the ECM algorithm. On the group level, a one-sample *t*-test was used to assess whether the difference between the centrality maps for high and low uncertainty were significantly greater than zero across participants. Resulting t-values were converted to z-scores and thresholded at $p < .001$ (10 contiguous voxels).

2.10.2. *Beta series correlation*

As a follow-up analysis on the ECM approach, we used a beta series correlation analysis (Rissman, Gazzaley, & D'Esposito, 2004) to assess trial-by-trial covariation of activity in our regions of interest. In short, trial-specific beta series within regions of interest (ROI) were correlated for each condition on the group level. For a step-by-step description of the analysis, the reader is referred to the Supplementary material.

3. Results

3.1. *Behavioural results*

3.1.1. *fMRI session*

Participants showed an overall high level of performance with a mean PR score of $M_{PR} = .89$ ($SD = .06$) during the fMRI session, indicating good attentiveness throughout the experiment. Out of 176 detectable sequences (not counting invalid cues), participants correctly responded to 165.73 events on average ($SD = 12.91$). Mean PR scores (Fig. 3A) did not differ

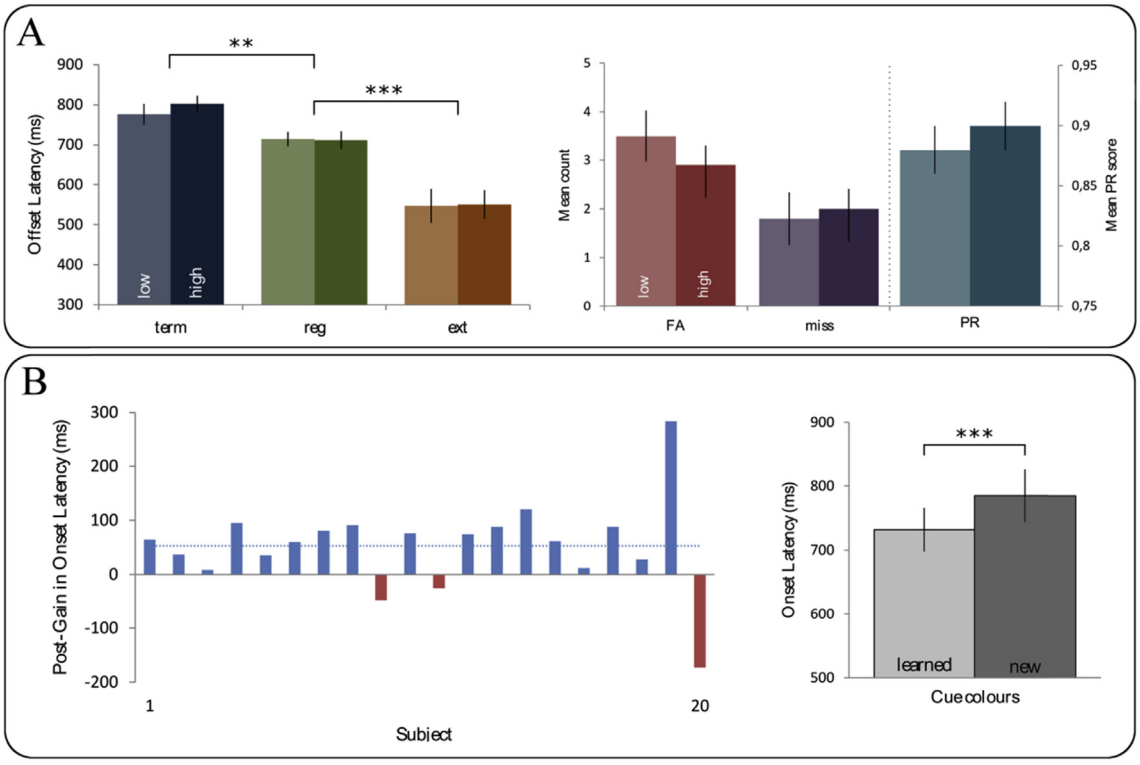

Fig. 3 – (A) Left panel: Effects of expectation compliance (terminated, regular, extended) and irreducible uncertainty (low, high) on mean offset latency. Right panel: Mean count of false alarms and misses as well as the mean PR score as a function of uncertainty. (B) Left panel: Differences in onset latency between new and learned cue colours during post-measurement for each subject. Blue bars indicate faster onset for learned cue colours, dotted line depicts mean gain across subjects. Right panel: Overall mean onset latency for learned and new cue colours, respectively. Error bars show standard error of the mean (SEM). ** = $p < .01$, *** = $p < .001$.

Table 1 – Activation peaks, z-values, and anatomical locations for the main effect of expectation compliance (TERM > EXT) and the conjunction of the two prediction error types versus checkpoints, respectively (TERM > CHECK ∩ EXT > CHECK).

Area	Local maxima				Volume (mm^3)
	MNI			z-value	
	x	y	z		
TERM > EXT					
Left IFG/BA44	−45	7	26	3.73	3402
Right PCG	36	−29	71	4.59	2916
EXT > TERM					
Right anterior SFS	27	58	23	−3.94	4212
Right STG	48	−5	−4	−4.13	2349
Right PCC/BA31	15	−32	41	−3.90	2025
Right BA40	60	−35	44	−4.85	11 394
Left BA7	−21	−62	71	−4.52	1512
Left STG	−51	1	−7	−4.46	5103
(TERM > CHECK) ∩ (EXT > CHECK)					
Right putamen	30	−5	−1	4.02	891

IFG = inferior frontal gyrus, BA = Brodmann Area, PCG = postcentral gyrus, SFS = superior frontal sulcus, STG = superior temporal gyrus, PCC = posterior cingulate cortex.

significantly between experimental blocks [$F(3, 76) = 1.23$, $p = .30$], nor as function of uncertainty [$t(21) = .21$, $p = .84$]. As stated above, two participants were excluded from further analyses due to their behavioural performance (standardised PR scores of $z_{PR} = -1.79$ and $z_{PR} = -2.47$, respectively).

The repeated-measures ANOVA yielded a significant main effect of expectation compliance on offset latency [$F(2, 38) = 45.75$, $p < .001$, Greenhouse-Geisser-corrected]. Post-hoc pairwise *t*-tests revealed participants' button releases to be significantly slower after terminated ($M = 783.72$ ms, $SD = 77.94$ ms) than after regular ($M = 713.92$ ms, $SD = 76.91$ ms, fdr-adjusted $p < .01$) as well as after extended sequences ($M = 549.94$ ms, $SD = 121.73$ ms, fdr-adjusted $p < .001$). The difference between extended and regular sequences was significant as well (fdr-adjusted $p < .001$). This pattern of offset latency differences appears intuitive in the sense that premature terminations unexpectedly violated the prediction of continued sequential input, thus inducing a delayed response compared to the regular condition. Critically, neither the main effect of uncertainty [$F(1, 19) = .16$, $p = .70$] nor the interaction term of *uncertainty X expectation compliance* [$F(2, 38) = .16$, $p = .85$] reached statistical significance, suggesting that participants were able to discriminate regular from manipulated sequences regardless of the respective level of uncertainty. The number of misses [$t(19) = -.58$, $p = .57$] and false alarms [$t(19) = .24$, $p = .81$] did not differ significantly between high and low uncertainty blocks (see Fig. 3A).

3.1.2. *Post-measurement*

Participants performed equally well during the post-measurement ($M_{PR} = .90$, $SD = .06$) as they had during the fMRI session. Out of 40 detectable sequences (not counting invalid cues), participants correctly responded to 38.77 ($SD = 2.02$) sequences on average.

The post-measurement was conducted in order to assess accessibility of the signalling information provided by the cues. If participants had learned the association of cue colours and prospective ordered sequences over the course of the training and the fMRI session, they were expected to react faster to sequences beginning with established cue colours than to those starting with new colours during the post-measurement. Indeed, the corresponding *t*-test confirmed a significant difference between learned and new cue colours [$t(19) = -2.78$, $p = .006$, one-tailed]. Participants exhibited a shorter reaction time (defined as onset latency relative to the second sequential stimulus, see above) to learned cue colours ($M = 731.76$ ms, $SD = 152.68$) than to new cue colours just introduced during the post-measurement ($M = 784.78$ ms, $SD = 184.04$; see Fig. 3B).

3.2. *fMRI results*

Supporting our first hypothesis, group-level activations discernibly related to sequential terminations (TERM > EXT) were found in left IFG. In contrast, sequential extensions (EXT > TERM) were found to be distinctly reflected in activations across an extensive network comprising posterior cingulate cortex (PCC), right superior frontal sulcus (SFS), and right angular gyrus (Table 1).

As expected, uncertainty had a significant effect on checkpoints processing (CHECK HIGH > CHECK LOW). Contrary to our hypothesis, however, enhanced activation at sequential checkpoints during blocks of high uncertainty was not found in ACC, but in right IFG and the corresponding projection area in parietal cortex, right angular gyrus/temporoparietal junction (rANG/TPJ, Fig. 4B; see Table 2 for coordinates).

The conjunction of terminations and extensions relative to checkpoints (i.e., unexpected relative to expected events, TERM > CHECK ∩ EXT > CHECK) yielded significant activation in the right putamen (Fig. 4C; see Table 2 for peak coordinates). Conceptually, this joint activation reflects the shared portion of prediction error processing (i.e., an unexpected violation of the internal model) in distinction to the qualitative differences in how the internal model is violated (i.e., having to prematurely neglect *vs* unexpectedly resume the sequence model, see above).

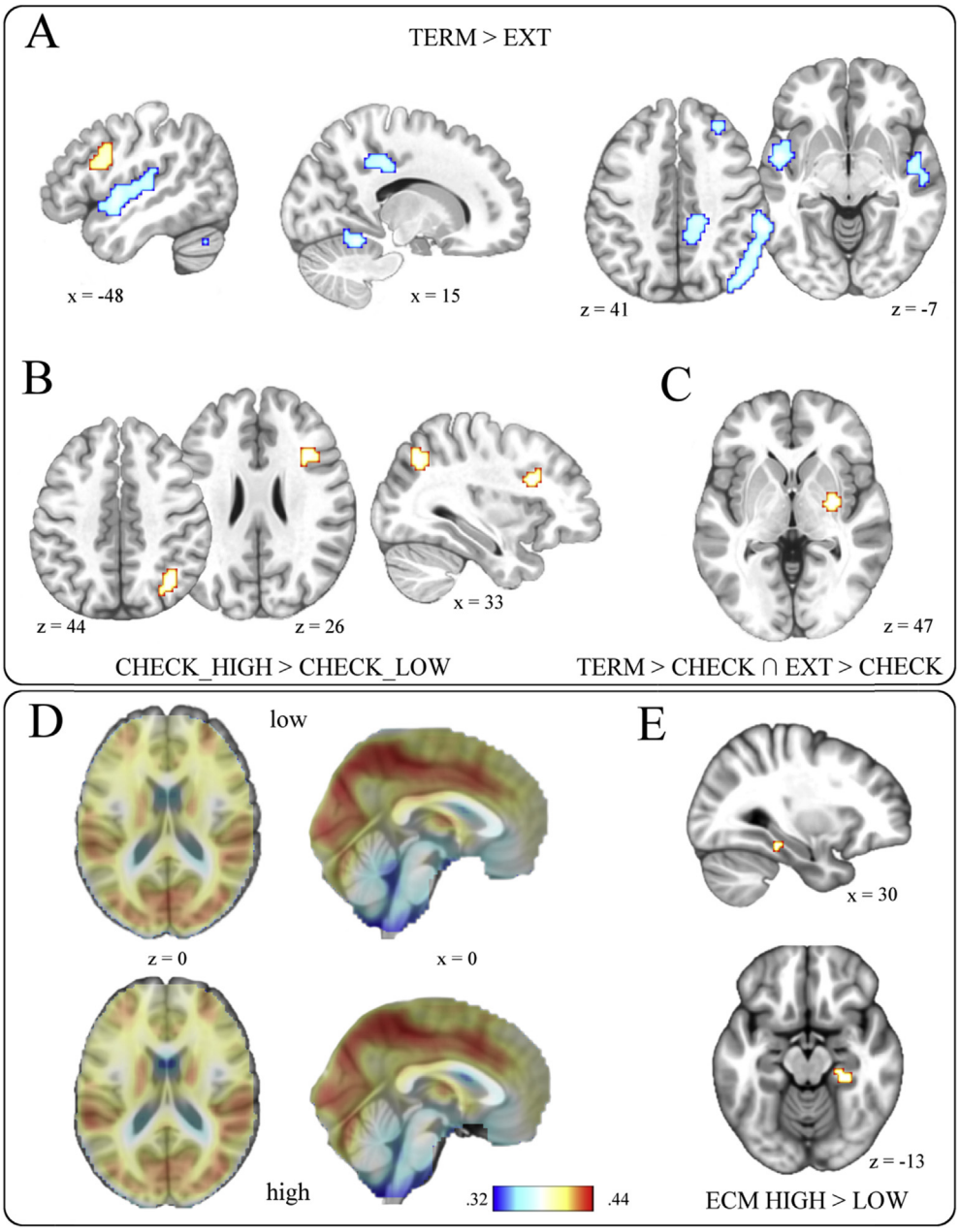

Fig. 4 – (A) Areas positively correlated with sequential terminations (red) and extensions (blue). (B) Areas reflecting neural processing at sequential checkpoints for high (*vs* low) uncertainty. (C) Common activations of terminations and extensions relative to checkpoints. (D) Group averages of eigenvector centrality for low and high uncertainty blocks. (E) Significantly higher centrality within the parahippocampal region for high > low uncertainty as revealed by a pairwise *t*-test.

The surprise parameter modulated neural responses in a widespread network (Table 2) including bilateral anterior-dorsal insular cortex, right ACC, and right fusiform gyrus (see Supplementary Fig. S2).

3.3. *Exploratory eigenvector centrality mapping*

Based on the finding that irreducible uncertainty modulated neural processing of sequential checkpoints, we used ECM as an exploratory tool to further analyse uncertainty effects. Adding to the reported modulations in BOLD amplitude, ECM as a measure of functional connectivity was employed to detect uncertainty-related differences on the neural network level.

Both high and low uncertainty conditions equally displayed a network of highly interconnected nodes including cingulate cortex, precuneus, basal ganglia, IFG, and visual areas (Fig. 4D). Intriguingly, significantly higher eigenvector centrality was observed in the right parahippocampal region (MNI coordinates 27, −35, −13) for the high uncertainty

Table 2 – Activation peaks, z-values, and anatomical locations for the effect of irreducible uncertainty on checkpoint processing (CHECK_HIGH > CHECK_LOW) and the parametric effect of surprise.

Area	local maxima				Volume (mm^3)
	MNI			z-value	
	x	y	z		
CHECK_HIGH > CHECK_LOW					
Right IFG/BA44	33	16	26	4.14	1377
Right TPJ/angular gyrus	36	−65	41	3.94	1458
SURPRISE					
Right dorsal insula	30	28	2	4.60	2781
Right ACC	0	13	29	3.74	1431
Right BA40	60	−44	26	3.77	1431
Right BA7	15	−47	65	3.67	837
Left dorsal insula	−42	10	−1	4.46	6183
Left BA4/BA6	−45	−8	56	3.97	891

IFG = inferior frontal gyrus, BA = Brodmann Area, TPJ = temporoparietal junction, ACC = anterior cingulate cortex.

condition, indicating stronger functional connections between parahippocampal areas and the other central nodes (see above) during time periods of statistical instability (Fig. 4E).

3.4. *Beta series correlation*

Significant trial-by-trial correlations between our regions of interest were found to be exclusively positive. Uncertainty-induced changes in network connectivity appear to differ between conditions: For terminations and extensions, there were several significant links between areas under high uncertainty that were absent under low uncertainty (see Fig. 5). This does not seem to be the case for checkpoints for which all network components were significantly correlated under low uncertainty. Parahippocampal (PHC) beta series under high uncertainty were found to be significantly correlated with those of virtually all other network components for terminations and checkpoints, but not for extensions. Moreover, whereas the increase in significant PHC connections for high > low uncertainty is most evident for terminations (with no significant correlation of PHC under low uncertainty), PHC was highly interconnected even under low uncertainty at checkpoints and thus showed no increase under high uncertainty. Finally, PHC was not significantly correlated with any other network component at extensions (under neither uncertainty level).

3.5. *Correlation of behavioural and functional data*

We hypothesised predictive processing to be adapted to statistical properties of environments (in this case, irreducible uncertainty). Conceivably, this strategic adaptation could manifest on the behavioural level – successful adaption to highly uncertain contexts should facilitate resolution of conflict under uncertainty and thus result in response time advantages at corresponding events. As we propose such adaptation to originate from more pronounced processing at checkpoints under high uncertainty, the uncertainty-related behavioural measures reported so far may very well have been too non-specific to reflect particular effects on reaction

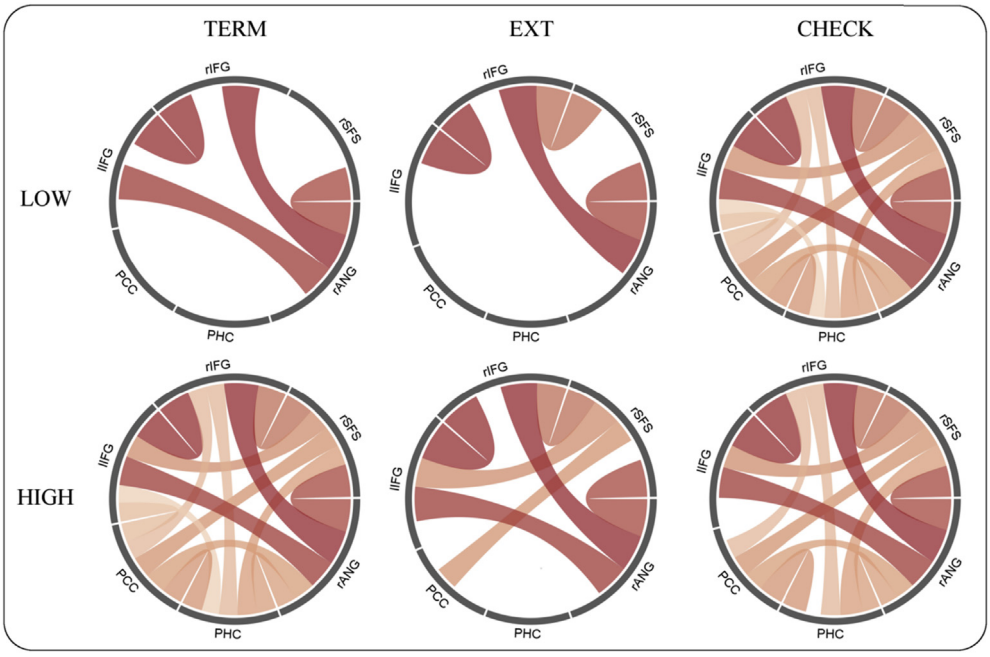

Fig. 5 – Connectivity patterns within the network identified in the fMRI contrasts. Significant correlations of trial-specific beta series for terminations (TERM), extensions (EXT), and checkpoints (CHECK) are shown for both low and high uncertainty. Links coloured in red depict positive correlations, with darker tone corresponding to higher r. lIFG = left inferior frontal gyrus, rIFG = right inferior frontal gyrus, rSFS = right superior frontal sulcus, rANG = right angular gyrus, PHC = parahippocampal cortex, PCC = posterior cingulate cortex.

times. To closely link behavioural measures to the reported BOLD effects, we correlated subject-level regression weights from the CHECK_HIGH > CHECK_LOW contrast (i.e., rIFG and rANG, see above) with individual differences in offset latency between high and low uncertainty blocks. Importantly, since checkpoints were exclusively sampled from regular sequences for the fMRI contrasts, equally did only button releases at the end of regular sequences contribute to the reported differences in the correlation analysis. Both rANG ($r(18) = .21$, $p = .19$, one-sided) and rIFG ($r(18) = .12$, $p = .31$, one-sided) were found to show a small but non-significant correlation with faster reaction times in highly uncertain blocks (Fig. 6A).

In a second brain-behaviour correlation analysis, we assessed whether individual differences in successful learning of the cue-length-contingency (operationalised as quicker reactions to learned *vs* new cue colours in the post measurement, see Fig. 3B) were differentially related to activity in rIFG and rANG (Fig. 6B). The difference between the two correlations ($r(18) = .35$, $p = .07$ and $r(18) = .12$, $p = .31$, one-sided) was found to be non-significant ($z = 1.01$, $p = .16$, one-tailed).

4. Discussion

The present fMRI study was conducted to investigate the strategic adaptation of predictive processing to different non-reward prediction error qualities and to the prediction's contextual uncertainty. Distinguishable activation patterns were elicited by prediction errors depending on the respective error type, lending support to a differential concept of non-reward prediction errors. In particular, we found that unexpected terminations and extensions of predicted stimulus regularities elicited increased activity in distinct brain networks. Moreover, increased activity at checkpoints for high versus low irreducible uncertainty suggests that context stability affects predictive strategies. Notably, this effect was controlled for the quantitatively variable surprise level (i.e., respective improbability) of the sampled event types. Potentially, stable (i.e., low uncertainty) contexts allowed a full-length prediction of sequential input based on the internal model, whereas highly uncertain contexts induced iterant comparisons of sensory information with the internal model. Neural processing at checkpoints was more pronounced in these unstable contexts, possibly pointing towards a stepwise (rather than full model length) prediction. Although further research is needed to link neural effects to changes on the behavioural level, these results provide novel insight into potentially adaptive prediction strategies and their respective neural underpinnings.

4.1. *Qualitative differences of prediction errors*

Predictions of digit sequences could be violated by termination or extension of the expected sequence length. While both types of prediction error (relative to checkpoints) commonly elicited enhanced activity in right-lateralised putamen, their direct contrast yielded distinct frontal/frontoparietal activity specific to the respective prediction error type. While we tested a specific hypothesis for this contrast (IFG for terminated sequences), we discuss further findings to suggest testable hypotheses for future studies.

Terminated sequences correlated with neural activity within IFG (BA44, see below) whereas extensions were reflected in effects along the anterior portion of right SFS (lateral BA8/9). Evidence from the action observation literature has implicated the SFS in the processing of event boundaries (Schubotz, Korb, Schiffer, Stadler, & von Cramon, 2012), i.e., behaviourally relevant transition points in event perception. In line with the authors' interpretation of boundary-related SFS activity as a correlate of updating attention to the next stimulus, prediction error signals caused by sequential extensions presumably reflect the violation of the (expected) sequence ending: at the point of a sequential extension, participants were presented an unpredicted sequential digit when in fact expecting a random digit denoting the end of the ordered sequence (vice versa for terminated sequences). In other words, present correlates of extended sequences supposedly express a prediction error signal that ultimately results in memory-directed reorientation of attention, i.e., the resumption of the internal model.

This interpretation is substantially supported by coactivation of the angular gyrus, another component frequently associated with attentional reorientation towards salient or informative stimuli (Gottlieb, 2007; Kincade, Abrams, Astafiev, Shulman, & Corbetta, 2005; Rushworth, Ellison, & Walsh, 2001). The angular gyrus, specifically the dorsal portion we report for sequential extensions, has been shown to be connected to superior frontal areas via the occipito-frontal fascicle (Makris et al., 2007; Nelson et al., 2010). Functionally, one suggested role for the angular gyrus in attentional updating has been the integration of current stimuli with recent task history (Taylor, Muggleton, Kalla, Walsh, & Eimer, 2011) – a highly relevant operation for extended but not for terminated sequences. In a similar vein, O'Connor, Han, and Dobbins (2010) reported expectancy violations in an attentional cueing task to be reflected in supramarginal and angular gyrus. Their differential findings of prediction errors following old versus new items led the authors to assume that inferior parietal lobe (IPL) lesions should affect cognitive control mechanisms especially when unexpected familiar items violate a strong expectation of novel stimuli. Our results further substantiate these suggestions, as the characteristic quality of extended sequences was precisely the observation of history-conform sequential digits when participants expected novel (i.e., random) digits.

In contrast to sequential extensions, *one specific* digit (i.e., the preceding number raised by one) was expected at the point of violation during terminated sequences. Therefore, sequential terminations can be considered violating a more specific prediction than was the case for sequential extensions. Our finding of IFG activity increase for sequential terminations adds to consistent reports of BA44 reflecting violations of expected regularities in language syntax (Friederici & Kotz, 2003), musical structure (Maess, Koelsch, Gunter, & Friederici, 2001), actions (Wurm & Schubotz, 2012), and abstract stimuli (Huettel, Mack, & McCarthy, 2002). Contrary to an unexpected *continuation* of observed regularities (see above), these studies and our own results commonly

point to a role for IFG in processing premature rule violations when regular input of certain specificity is expected.

4.2. *Predictive processing as a function of statistical context*

The second main aim of the present study was to assess predictive strategies in varying statistical contexts. Processing of changes in statistical regularities per se has been demonstrated for both reward (Behrens et al., 2007) and non-reward paradigms (Tobia, Iacovella, Davis, & Hasson, 2012). However, it remains unclear whether or not predictions of abstract upcoming input strategically change with context (note that here, "strategically" does not imply a conscious effort). To dissociate predictions in a stable versus unstable context, the reasoning was as follows: while an implicit cue might trigger the prediction of sequential input at full length in a stable context, an unstable context might lead to a stepwise processing confirming the prediction is still valid. Recall the staircase analogy from before: in an unstable context (e.g., in dim lighting), one might be well advised to verify the initial prediction ("This flight has 13 steps") at some critical point in order not to encounter a (potentially precarious) prediction error.

Following this rationale, we investigated effects of irreducible uncertainty on the neural processing of possible checkpoints during prediction. Checkpoints were defined as regular events at those sequential positions where prediction errors occurred in terminated or extended sequences. Note that, by definition, violations of the cue – length contingency did not occur in regular sequences from which checkpoints were sampled. Right IFG showed increased BOLD activity at checkpoints within the high (*vs* low) uncertainty condition. Given the central involvement of prefrontal cortex (PFC) in flexible interactions with the environment, a process oftentimes termed *cognitive control* (Corbetta & Shulman, 2002; Petrides, 2000), enhanced prefrontal responses at *potential* violation sites might indeed be interpreted as an updating mechanism accounting for changes of statistical regularities. Previous work has shown that experimental context can be decoded from prefrontal neurons (Waskom, Kumaran, Gordon, Rissman, & Wagner, 2014), suggesting that cognitive control and decision-making benefit from representations of current context encoded in PFC. Conceivably, the use of specific versus higher-order information for context encoding in PFC depends on the respective network in which frontal sites are coactivated. Recall that left-lateralised IFG activation was found for violations of number-specific expectations: Consolidating IFG effects for both sequential terminations and highly uncertain checkpoints, the common role for prefrontal sites may be a close monitoring of structured incoming information. Depending on whether these monitoring processes lead to the detection of a specific prediction error (as in the TERM > EXT contrast) or provide vital information about the current task context (i.e., CHECK_HIGH > CHECK_LOW), respective network partners are coactivated accordingly. Support for this interpretation comes from our finding that checkpoint processing under high uncertainty was also found to be reflected within the right angular gyrus/TPJ. As a direct projection site of IFG, TPJ has been established as part of a ventral network engaged in attentional control (Corbetta & Shulman, 2002; see Cabeza, Ciaramelli, Olson, & Moscovitch, 2008 for a review). Specifically, this network initiates a bottom-up reorientation driven by behaviourally relevant but unattended stimuli. Fittingly, demanding the actor to enter a special attentional mode is one characteristic of junctures from the field of sequential action selection (*decision points*; Reason, 1992). This way, increased allocation of attentional resources may be one plausible interpretation of rANG/TPJ effects for high uncertainty checkpoints. However, an intriguing hypothesis redefining TPJ function was put forward by Geng and Vossel (2013): the authors propose contextual updating as the main role of TPJ in cognitive processing, meaning the updating of internal models of context based on new sensory information (Seghier, 2013). It is important to recall that the contrast of interest (*CHECK_HIGH > CHECK_LOW*) only contained events of regular sequences where a violation of prediction (termination or extension, respectively) was probable but did in fact not occur. Since there was no external signal initiating a change in predictive strategies, enhanced processing of checkpoints for highly uncertain contexts was solely based on the internal sequence model developed through previous experience. Consequently, contextual updating as well as corresponding strategic adjustments (i.e., the use of incremental predictions in unstable environments) do not seem to require a bottom-up trigger signal but can instead be prompted by model-based expectancies alone. This suggests an extension of the understanding of TPJ functioning for paradigms where contextual updating relies on top-down generated internal models of context.

Due to the higher average surprise value for checkpoints in high versus low uncertainty blocks, an increase in surprise could potentially present an intuitive explanation for the reported results. Crucially, however, since the surprise parameter was modelled separately within the GLM, our findings cannot be attributed to stimulus-bound surprise but instead reflect higher-order cognitive processes exceeding trial-by-trial variation in informational value.

In sum, elevated BOLD responses within rIFG and rANG at sequential checkpoints potentially point to an adaptive quality of abstract predictive processing that to our knowledge has not been demonstrated. Depending on the stability of statistical contexts, the top-down predictive strategy may vary with regard to how far expectations reach into the future. Supporting this interpretation on the behavioural level, the extent to which participants learned the colour-length association (i.e., their gain in response speed during post-measurement) was more strongly correlated with the BOLD uncertainty effects in the frontal (rIFG) than in the parietal (rANG) component of the checkpoint network (although the difference in correlation did not reach significance). In other words, especially for rIFG, the more successful the contingency between cue colour and sequence length was learned, the more pronounced was the neural activity at checkpoints under high uncertainty (see Fig. 6).

Motivated by the reported BOLD amplitude effects of uncertainty, exploratory functional connectivity analysis (i.e., ECM) revealed eigenvector centrality of the right middle temporal gyrus (MTG)/parahippocampal region (PHC) to

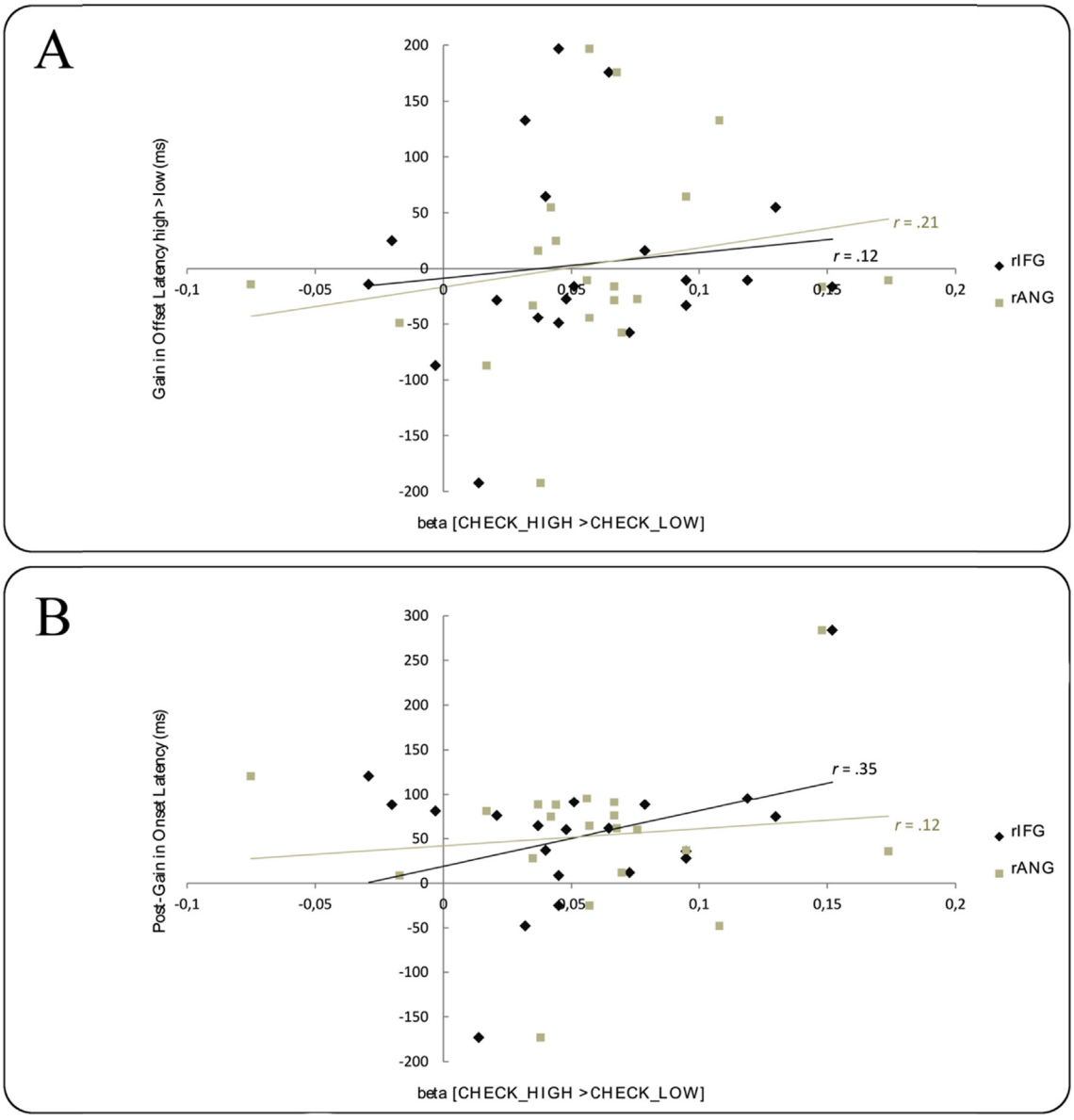

Fig. 6 – (A) Correlation of beta weights extracted from the contrast of high versus low uncertainty checkpoints and the difference in offset latency following regular sequences in high versus low uncertainty environments. Differences in offset latency are depicted as gain under high uncertainty, i.e., faster reaction times for button releases at the end of regular sequences under high (*vs* low) uncertainty. (B) Correlation of beta weights extracted from the contrast of high versus low uncertainty checkpoints and the difference in onset latency for learned versus new cue colours during the post test. Differences in onset latency are depicted as 'gain during post measurement', i.e., faster reaction times for button presses at the beginning of ordered sequences following learned (*vs* new) cue colours.

increase during epochs of high uncertainty. This reflects a strengthened connectivity between the parahippocampal region and those highly interconnected frontoparietal circuits that are central for the currently employed task. More detailed analyses of trial-specific beta series within our regions of interest (see Supplementary material) suggest differential connectivity patterns of PHC depending on the outcome of a sequence and the respective level of uncertainty: While PHC was found to be highly interconnected at checkpoints (regardless of uncertainty), the same level of connectivity was found only for high uncertainty terminations. Lastly, PHC activity at extensions did not covary significantly with any other network component. One possible hypothesis would be that representations of terminations and checkpoints could be more similar than, say, terminations and extensions; an intriguing starting point for multivariate assessment of event characteristics such as representational similarity analysis (RSA, Kriegeskorte, Mur, & Bandettini, 2008). Another

possibility would be to look at network configurations at different points in time and formulate hypotheses about graph measures (e.g., network density) to learn more about the respective roles of key regions implicated in predictive processing under uncertainty. These results motivate intriguing hypotheses and objectives for future research targeting network configuration as a function of uncertainty (see Limitations and future directions).

The medial temporal lobe including the hippocampal formation has been established as a crucial structure for prospective processing and pattern completion during perception (Turk-Browne, Scholl, Johnson, & Chun, 2010), sequence learning (Schapiro, Gregory, Landau, McCloskey, & Turk-Browne, 2014; Schendan, Searl, Melrose, & Stern, 2003), and especially at points of ambiguity (Bornstein & Daw, 2012; Kumaran & Maguire, 2006; Ross, Brown, & Stern, 2009). When multiple competing predictions with regard to the next sequential item arise under uncertainty, the MTG network is hypothesised to resolve this ambiguity, resulting in enhanced hippocampal responses (for a review, see Davachi & DuBrow, 2015). Critically, the present high uncertainty condition was hypothesised to intensify neural processing at ambiguous checkpoints by means of a higher proportion of sequential deviants. Therefore, the finding of strengthened functional connectivity between the parahippocampal region and central task-related structures in a highly uncertain environment further corroborates the understanding of MTG as a contingency-sensitive circuitry engaged in encoding and extracting statistical information. Our results moreover suggest that this information could then be employed to facilitate a context-appropriate change in predictive processing, namely a stepwise prediction strategy for highly uncertain contexts. This way, instability in the environment could supposedly be compensated by more frequently comparing model-based expectations with actual sensory input. Combining the contextual updating hypothesis and MTG involvement in sequential ambiguity, enhanced overall connectivity of MTG/parahippocampus under high uncertainty could thus be interpreted as evaluating the validity of top-down, model-based predictions in light of incoming sensory information (Kumaran & Maguire, 2006; Lisman, 1999). Presumably, a stepwise prediction is not necessary in stable contexts, possibly due to frequent validation of the internal model (i.e., the high proportion of regular sequences) resulting in high confidence in the initial full-length prediction. As for computational efficiency and economic processing, stepwise prediction would appear to be a strategic adaptation to unstable contexts in order to avoid the cost of prediction errors. One intuitive neural implementation of these stepwise predictions would be through enhanced communication between MTG and frontoparietal networks, thus enabling recourse to model information in working memory. Indeed, previous studies have demonstrated the anatomical connectivity between angular gyrus/TPJ, associated frontal areas (IFG/lateral PFC), and MTG (Clower, West, Lynch, & Strick, 2001; Makris et al., 2005; Petrides & Pandya, 1999; Vincent et al., 2006). Within the scope of the contextual updating hypothesis, these connections are thought to integrate internal representations of current context information with the appropriate sensorimotor transformation necessary to respond adequately (Geng & Vossel, 2013). Strengthened MTG involvement in contexts where regular updating is beneficial suggests that the internal model is iteratively checked based on cue information retrieved from working memory.

4.3. *Limitations and future directions*

The present study, conceptualised as a first step into investigating adaptive qualities in predictive processing, does not come without limitations. As mentioned above, one critical objective for future efforts is to replicate the differential effects for terminations and extensions in an experimental design that ensures equal response requirements for both PE types. Even though the direct contrast (TERM > EXT) does not contain components primarily associated with motor function, identical behavioural correlates would allow further analyses of response patterns, e.g., assessing modulatory effects of surprise on offset latency. Furthermore, subsequent efforts could aim to uncouple terminations and extensions from fixed sequential positions, thus eliminating potential influence of timing or sequence length. Future directions also include the use of multivariate approaches, as single run measurement of fMRI data limited the applicability of multivariate analyses for our present study. Follow-up studies could then use tools such as RSA to decode neural representations of the internal model at different points in time (see Schuck et al., 2015 for preparatory mPFC encoding prior to strategy change). Such multivariate approaches could also be combined with electroencephalography data (EEG, currently in preparation) to provide novel information on the time course of representations as a function of statistical context.

5. Conclusion

Different classes of abstract prediction errors were reflected in distinct brain activation patterns, predominantly within separate frontoparietal networks. Depending on whether the respective prediction error called for reorienting towards external stimuli or staying with the internal model, cognitive processing was adjusted accordingly. High irreducible uncertainty resulted in more pronounced processing of sequential checkpoints we preliminarily interpret as iterative comparisons of sensory information and the internal model. Although further research is needed, our findings suggest that this stepwise predictive strategy may be conducted through enhanced connectivity between frontoparietal circuits and the (para-)hippocampal area.

Acknowledgements

We would like to thank Christiane Ahlheim, Laura Quante, Ima Trempler, and Leon Windscheid for their valuable comments on earlier drafts of this manuscript, as well as Sarah Fromme, Irina Kaltwasser, and Monika Mertens for their help during data collection. Finally, we are thankful for the insightful and productive comments by our reviewers.

Supplementary data

Supplementary data related to this article can be found at https://doi.org/10.1016/j.cortex.2017.09.017.

REFERENCES

Allen, T. A., Salz, D. M., McKenzie, S., & Fortin, N. J. (2014). Nonspatial sequence coding in CA1 neurons. *Journal of Neuroscience, 36*, 1547–1563.

Bastos, A. M., Usrey, W. M., Adams, R. A., Mangun, G. R., Fries, P., & Friston, K. J. (2012). Canonical microcircuits for predictive coding. *Neuron, 76*, 695–711.

Bayer, H. M., & Glimcher, P. W. (2005). Midbrain dopamine neurons encode a quantitative reward prediction error signal. *Neuron, 47*, 129–141.

Behrens, T. E. J., Woolrich, M. W., Walton, M. E., & Rushworth, M. F. S. (2007). Learning the value of information in an uncertain world. *Nature Neuroscience, 10*, 1214–1221.

Benjamini, Y., & Hochberg, Y. (1995). Controlling the false discovery rate: A practical and powerful approach to multiple testing. *Journal of the Royal Statistical Society Series B, 57*, 289–300.

Bland, A. R., & Schaefer, A. (2012). Different varieties of uncertainty in human decision making. *Frontiers in Neuroscience, 6*, 85.

Bonacich, P. (2007). Some unique properties of eigenvector centrality. *Social Networks, 29*, 555–564.

Bornstein, A. M., & Daw, N. D. (2012). Dissociating hippocampal and striatal contributions to sequential prediction learning. *European Journal of Neuroscience, 35*, 1011–1023.

Cabeza, R., Ciaramelli, E., Olson, I. R., & Moscovitch, M. (2008). The parietal cortex and episodic memory: An attentional account. *Nature Reviews Neuroscience, 9*, 613–625.

Clark, A. (2013). Whatever next? Predictive brains, situated agents, and the future of cognitive science. *Behavioral and Brain Sciences, 36*, 181–204.

Clower, D. M., West, R. A., Lynch, J. C., & Strick, P. L. (2001). The inferior parietal lobule is the target of output from the superior colliculus, hippocampus, and cerebellum. *Journal of Neuroscience, 21*, 6283–6291.

Corbetta, M., & Shulman, G. L. (2002). Control of goal-directed and stimulus-driven attention in the brain. *Nature Reviews Neuroscience, 3*, 201–215.

Davachi, L., & DuBrow, S. (2015). How the hippocampus preserves order: The role of prediction and context. *Trends in Cognitive Sciences, 19*, 92–99.

De Berker, A., Rutledge, R. B., Mathys, C., Marshall, L., Cross, G., Dolan, R., et al. (2016). Computations of uncertainty mediate acute stress responses in humans. *Nature Communications, 7*, 10996.

Delgado, M. R., Locke, H. M., Stenger, V. A., & Fiez, J. A. (2003). Dorsal striatum responses to reward and punishment: Effects of valence and magnitude manipulations. *Cognitive, Affective, & Behavioral Neuroscience, 3*, 27–38.

Den Ouden, H. E. M., Daunizeau, J., Roiser, J., Friston, K. J., & Stephan, K. E. (2010). Striatal prediction error modulates cortical coupling. *Journal of Neuroscience, 30*, 3210–3219.

Den Ouden, H. E. M., Friston, K. J., Daw, N. D., McIntosh, A. R., & Stephan, K. E. (2009). A dual role for prediction error in associative learning. *Cerebral Cortex, 19*, 1175–1185.

Egner, T., Monti, J. M., & Summerfield, C. (2010). Expectation and surprise determine neural population responses in the ventral visual stream. *Journal of Neuroscience, 30*, 16601–16608.

Fiebach, C. J., & Schubotz, R. I. (2006). Dynamic anticipatory processing of hierarchical sequential events: A common role for Broca's area and ventral premotor cortex across domains? *Cortex, 42*, 499–502.

Forman, S. D., Cohen, J. D., Fitzgerald, M., Eddy, W. F., Mintun, M. A., & Noll, D. C. (1995). Improved assessment of significant activation in function magnetic resonance imaging (fMRI): Use of a cluster-size threshold. *Magnetic Resonance in Medicine, 33*, 636–647.

Fortin, N. J., Agster, K. L., & Eichenbaum, H. B. (2002). Critical role of the hippocampus in memory for sequences of events. *Nature Neuroscience, 5*, 458–462.

Friederici, A. D., & Kotz, S. A. (2003). The brain basis of syntactic processes: Functional imaging and lesion studies. *NeuroImage, 20*, 8–17.

Friston, K. J. (2005). A theory of cortical responses. *Philosophical Transactions of the Royal Society of London B: Biological Sciences, 360*, 815–836.

Geng, J. J., & Vossel, S. (2013). Re-evaluating the role of TPJ in attentional control: Contextual updating? *Neuroscience & Biobehavioral Reviews, 37*, 2608–2620.

Gottlieb, J. (2007). From thought to action: The parietal cortex as a bridge between perception, action, and cognition. *Neuron, 53*, 9–16.

Harrison, L. M., Duggins, A., & Friston, K. J. (2006). Encoding uncertainty in the hippocampus. *Neural Networks, 19*, 535–546.

Holroyd, C. B., & Coles, M. G. H. (2002). The neural basis of human error processing: Reinforcement learning, dopamine, and the error-related negativity. *Psychological Review, 4*, 679–709.

Huettel, S. A., Mack, P. B., & McCarthy, G. (2002). Perceiving patterns in random series: Dynamic processing of sequence in prefrontal cortex. *Nature Neuroscience, 5*, 485–490.

Ishihara, S. (1917). *Test for colour-blindness*. Tokyo: Hongo Harukicho.

Jones, D. S. (1979). *Elementary information theory*. Oxford: Oxford University Press.

Kincade, J. M., Abrams, R. A., Astafiev, S. V., Shulman, G. L., & Corbetta, M. (2005). An event-related functional magnetic resonance imaging study of voluntary and stimulus-driven orienting of attention. *Journal of Neuroscience, 25*, 4593–4604.

Kriegeskorte, N., Mur, M., & Bandettini, P. (2008). Representational similarity analysis – Connecting the branches of systems neuroscience. *Frontiers, 2*, 1–28.

Kumaran, D., & Maguire, E. A. (2006). An unexpected sequence of events: Mismatch detection in the human hippocampus. *PLoS Biology, 4*, e424.

Lisman, J. E. (1999). Relating hippocampal circuitry to function: Recall of memory sequences by reciprocal dentate-CA3 interactions. *Neuron, 22*, 233–242.

Lisman, J. E., & Redish, A. D. (2009). Prediction, sequences and the hippocampus. *Philosophical Transactions of the Royal Society of London B: Biological Sciences, 364*, 1193–1201.

Lohmann, G., Margulies, D. S., Horstmann, A., Pleger, B., Lepsien, J., Goldhahn, D., et al. (2010). Eigenvector centrality mapping for analyzing connectivity patterns in fMRI data of the human brain. *PLoS One, 5*, e10232.

Lohmann, G., Müller, K., Bosch, V., Mentzel, H., Hessler, S., Chen, L., et al. (2001). Lipsia—A new software system for the evaluation of functional magnetic resonance images of the human brain. *Computerized Medical Imaging and Graphics, 25*, 449–457.

Maess, B., Koelsch, S., Gunter, T. C., & Friederici, A. D. (2001). Musical syntax is processed in Broca's area: An MEG study. *Nature Neuroscience, 4*, 540–545.

Makris, N., Kennedy, D. N., McInerney, S., Sorensen, A. G., Wang, R., Caviness, J. V. S., et al. (2005). Segmentation of subcomponents within the superior longitudinal fascicle in

humans: A quantitative, in vivo, DR-MRI study. *Cerebral Cortex, 15*, 854–869.
Makris, N., Papadimitriou, G. M., Sorg, S., Kennedy, D. N., Caviness, J. V. S., & Pandya, D. N. (2007). The occipitofrontal fascicle in humans: A quantitative, in vivo, DT-MRI study. *NeuroImage, 37*, 1100–1111.
Mumford, D. (1992). On the computational architecture of the neocortex. *Biological Cybernetics, 66*, 241–251.
Nelson, S. M., Cohen, A. L., Power, J. D., Wig, G. S., Miezin, F. M., Wheeler, M. E., et al. (2010). A parcellation scheme for human left lateral parietal cortex. *Neuron, 67*, 156–170.
Norman, D. A. (1981). Categorization of action slips. *Psychological Review, 88*, 1–15.
O'Connor, A. R., Han, S., & Dobbins, I. G. (2010). The inferior parietal lobule and recognition memory: Expectancy violation or successful retrieval? *Journal of Neuroscience, 30*, 2924–2934.
O'Reilly, J. X., Schüffelgen, U., Cuell, S. F., Behrens, T. E. J., Mars, R. B., & Rushworth, M. F. S. (2013). Dissociable effects of surprise and model update in parietal and anterior cingulate cortex. *Proceedings of the National Academy of Sciences of the United States of America, 38*, 3660–3669.
Payzan-LeNestour, E., & Bossaerts, P. (2011). Risk, unexpected uncertainty, and estimation uncertainty: Bayesian learning in unstable settings. *PLoS Computational Biology, 7*, 1–14.
Petrides, M. (2000). Mapping prefrontal cortical systems for the control of cognition. In A. W. Toga, & J. C. Mazziotta (Eds.), *Brain mapping: The systems* (pp. 159–176). San Diego: Academic Press.
Petrides, M., & Pandya, D. N. (1999). Dorsolateral prefrontal cortex: Comparative cytoarchitectonic analysis in the human and the macaque brain and corticocortical connection patterns. *European Journal of Neuroscience, 11*, 1011–1036.
Rao, R. P. N., & Ballard, D. H. (1999). Predictive coding in the visual cortex: A functional interpretation of some extra-classical receptive-field effects. *Nature Neuroscience, 2*, 79–87.
Reason, J. T. (1992). Cognitive underspecification: Its varieties and consequences. In B. J. Baars (Ed.), *Experimental slips and human error: Exploring the architecture of volition* (pp. 71–91). New York: Plenum.
Rissman, J., Gazzaley, A., & D'Esposito, M. (2004). Measuring functional connectivity during distinct stages of a cognitive task. *Neuroimage, 23*, 752–763.
Rolls, E. T. (2013). The mechanisms for pattern completion and pattern separation in the hippocampus. *Frontiers in Systems Neuroscience, 7*, 74.
Ross, R. S., Brown, T. I., & Stern, C. E. (2009). The retrieval of learned sequences engages the hippocampus: Evidence from fMRI. *Hippocampus, 19*, 790–799.
Rushworth, M. F. S., Ellison, A., & Walsh, V. (2001). Complementary localization and lateralization of orienting and motor attention. *Nature Neuroscience, 4*, 656–661.
Schapiro, A. C., Gregory, E., Landau, B., McCloskey, M., & Turk-Browne, N. B. (2014). The necessity of the medial temporal lobe for statistical learning. *Journal of Cognitive Neuroscience, 26*, 1736–1747.
Schendan, H. E., Searl, M. M., Melrose, R. J., & Stern, C. E. (2003). An fMRI study of the role of the medial temporal lobe in implicit and explicit sequence learning. *Neuron, 37*, 1013–1025.
Schiffer, A. M., Ahlheim, C., Wurm, M. F., & Schubotz, R. I. (2012). Surprised at all the entropy: Hippocampal, caudate and midbrain contributions to learning from prediction errors. *PloS One, 7*, e36445.
Scholl, J., Kolling, N., Nelissen, N., Stagg, C. J., Harmer, C. J., & Rushworth, M. F. S. (2017). Excitation and inhibition in anterior cingulate predict use of past experiences. *eLIFE, 6*, e20365.
Schubotz, R. I., Korb, F. M., Schiffer, A. M., Stadler, W., & von Cramon, D. Y. (2012). The fraction of an action is more than a movement: Neural signatures of event segmentation in fMRI. *Neuroimage, 61*, 1195–1205.
Schuck, N. W., Gaschler, R., Wenke, D., Heinzle, J., Frensch, P. A., Haynes, J. D., et al. (2015). Medial prefrontal cortex predicts internally driven strategy shifts. *Neuron, 86*, 331–340.
Schultz, W. (1998). Predictive reward signal of dopamine neurons. *Journal of Neurophysiology, 80*, 1–27.
Seghier, M. (2013). The Angular Gyrus: Multiple functions and multiple subdivisions. *Neuroscientist, 19*, 43–61.
Silvetti, M., Seurinck, R., & Verguts, T. (2013). Value and prediction error estimation account for volatility effects in ACC: A model-based fMRI study. *Cortex, 49*, 1627–1635.
Snodgrass, J. G., & Corwin, J. (1988). Pragmatics of measuring recognition memory: Applications to dementia and amnesia. *Journal of Experimental Psychology, 117*, 34.
Strange, B. A., Duggins, A., Penny, W., Dolan, R. J., & Friston, K. J. (2005). Information theory, novelty and hippocampal responses: Unpredicted or unpredictable? *Neural Networks, 18*, 225–230.
Taylor, P. C. J., Muggleton, N. G., Kalla, R., Walsh, V., & Eimer, M. (2011). TMS of the right angular gyrus modulates priming of pop-out in visual search: Combined TMS-ERP evidence. *Journal of Neurophysiology, 106*, 3001–3009.
Tobia, M. J., Iacovella, V., Davis, B., & Hasson, U. (2012). Neural systems mediating recognition of changes in statistical regularities. *NeuroImage, 63*, 1730–1742.
Turk-Browne, N. B., Scholl, B. J., Johnson, M. K., & Chun, M. M. (2010). Implicit perceptual anticipation triggered by statistical learning. *Journal of Neuroscience, 30*, 11177–11187.
Vincent, J. L., Snyder, A. Z., Fox, M. D., Shannon, B. J., Andrews, J. R., Raichle, M. E., et al. (2006). Coherent spontaneous activity identifies a hippocampal-parietal memory network. *Journal of Neurophysiology, 96*, 3517–3531.
Waskom, M. L., Kumaran, D., Gordon, A. M., Rissman, J., & Wagner, A. D. (2014). Frontoparietal representations of task context support the flexible control of goal-directed cognition. *Journal of Neuroscience, 34*, 10743–10755.
Wurm, M. F., & Schubotz, R. I. (2012). Squeezing lemons in the bathroom: Contextual information modulates action recognition. *NeuroImage, 59*, 1551–1559.
Yu, A. J., & Dayan, P. (2005). Uncertainty, neuromodulation, and attention. *Neuron, 46*, 681–692.